IL NUOVO CIMENTO Vol. 34 C, N. 1 Gennaio-Febbraio 2011
DOI 10.1393/ncc/i2011-10806-1

Colloquia: IFA 2010

Low-dose effects of ionizing radiations in *in vitro* and *in vivo* biological systems: A multi-scale approach study

A. Antoccia[1], E. Argazzi[2], M. Balata[3], R. Bedogni[4], F. Berardinelli[1], G. Bisogni[5][6], M. Bono[2], U. Bottigli[5][7], A. Brunetti[8][9], A. Buttafava[10], G. Castellani[11], F. Centis[12], W. Cesarini[2][3], R. Cherubini[13](*), A. Cossu[14], G. Cugia[3][15], M. Dattena[16], V. De Nadal[13], D. Dondi[10], A. Esposito[4], A. Faucitano[10], P. L. Fiori[14], E. Fusco[17], S. Gerardi[13], M. Laubenstein[3], A. Lucarini[15][18], M. Marengo[11][19], G. L. Masala[8], D. Nieri[1], S. Nisi[3], F. Picardi[20], G. Pintus[14], A. Posadino[14], P. Randaccio[21][9], D. Remondini[11], A. Sgura[1], S. Stramigioli[12], C. Tanzarella[1], M. Valentini[12], L. Zamai[3][15], G. Zini[3] and I. Zironi[11]

([1]) *INFN, Sezione di Roma 3 and Dipartimento di Biologia, Università di Roma 3 Rome, Italy*
([2]) *SOC Fisica Medica, AO San Salvatore - Pesaro, Italy*
([3]) *INFN, Laboratori Nazionali del Gran Sasso - Assergi (AQ), Italy*
([4]) *INFN, Laboratori Nazionali di Frascati - Frascati (RM), Italy*
([5]) *INFN, Sezione di Pisa - Pisa, Italy*
([6]) *Dipartimento di Fisica, Università di Pisa - Pisa, Italy*
([7]) *Dipartimento di Fisica, Università di Siena - Siena, Italy*
([8]) *Struttura Dipartimentale di Matematica e Fisica, Università di Sassari - Sassari, Italy*
([9]) *INFN, Sezione di Cagliari - Cagliari, Italy*
([10]) *Dipartimento di Chimica Generale, Università di Pavia and INFN, Sezione di Pavia Pavia, Italy*
([11]) *Dipartimento di Fisica, Università di Bologna and INFN, Sezione di Bologna Bologna, Italy*
([12]) *Laboratorio di Patologia Clinica, AO San Salvatore - Pesaro, Italy*
([13]) *INFN, Laboratori Nazionali di Legnaro - Legnaro (PD), Italy*
([14]) *Dipartimento di Scienze Biomediche, Università di Sassari - Sassari, Italy*
([15]) *Dipartimento SUAN, Università di Urbino "Carlo Bo" - Urbino, Italy*
([16]) *AGRIS Sardegna, Settore scientifico riproduzione - Sassari, Italy*
([17]) *UOC di Ginecologia Zona Territoriale 2 - Urbino, Italy*
([18]) *ASLEM - San Marino, Repubblica di San Marino*
([19]) *Sezione di Fisica Sanitaria Policlinico S. Orsola - Bologna, Italy*
([20]) *Servizio di Medicina Trasfusionale, AO San Salvatore - Pesaro, Italy*
([21]) *Dipartimento di Fisica, Università di Cagliari - Cagliari, Italy*

(ricevuto il 30 Luglio 2010; approvato il 31 Agosto 2010; pubblicato online il 15 Febbraio 2011)

(*) E-mail: roberto.cherubini@lnl.infn.it

Summary. — Long-term biological effects of low-dose radiation are little known nowadays and its carcinogenic risk is estimated on the assumption that the risk remains linearly proportional to the radiation dose down to low-dose levels. However in the last 20 years this hypothesis has gradually begun to seem in contrast with a huge collection of experimental evidences, which has shown the presence of a plethora of non-linear phenomena (including hypersensitivity and induced radioresistance, adaptive response, and non-targeted phenomena like bystander effect and genomic instability) occurring after low-dose irradiation. These phenomena might imply a non-linear behaviour of cancer risk curves in the low-dose region and question the validity of the Linear No-Threshold (LNT) model currently used for cancer risk assessment through extrapolation from existing high-dose data. Moreover only few information is available regarding the effects induced on cryopreserved cells by multi-year background radiation exposure, which might induce a radiation-damage accumulation, due to the inhibition of cellular repair mechanisms. In this framework, the multi-year EXCALIBUR (*EXposure effeCts At Low doses of Ionizing radiation in Biological CultURes*) experiment, funded by INFN-CNS5, has undertaken a multi-scale approach investigation on the biological effects induced in *in vitro* and *in vivo* biological systems, in culture and cryopreserved conditions, as a function of radiation quality (X/γ-rays, protons, He-4 ions of various energies) and dose, with particular emphasis on the low-dose region and non-linear phenomena, in terms of different biological endpoints.

PACS `87.53.-j` – Effects of ionizing radiation on biological systems.
PACS `87.53.Ay` – Biophysical mechanisms of interaction.
PACS `87.53.Bn` – Dosimetry/exposure assessment.
PACS `87.18.Gh` – Cell-cell communication; collective behavior of motile cells.

1. – Introduction

Natural background radiation is estimated to be 1–3 mSv/year [1], depending on the specific geographic areas. At this dose level, ionizing charged particles and γ-rays daily hit only $\approx 1\%$ of the 100 trillion cells that make up the average human body. These collisions generate clusters of secondary electrons and free radicals, known as reactive oxygen species, with different energetic and spatial distributions depending on radiation quality (type and energy), that randomly damage cellular constituents including DNA. At the other end of the scale, acute exposures of above 200–500 mSv, a range known as high-dose radiation, have measurable and often serious immediate effects on humans that can be determined directly from available epidemiological data. Between background and high-dose radiation is the range of exposures known as low-dose radiation (below 0.5 Gy). Long-term biological effects of low-dose radiation are little known nowadays and its carcinogenic risk is estimated under the assumption that the risk remains linearly proportional to the radiation dose down to low-dose levels. This would imply that the biological effects of high and low doses are mediated by the same mechanisms. This hypothesis seems to be in contrast with a huge body of experimental evidences collected in the last 20 years, which has shown the presence of a plethora of non-linear phenomena (including hypersensitivity and induced radioresistance, adaptive response, and non-targeted phenomena like bystander effect and genomic instability) occurring

after low-dose irradiation. These phenomena might imply a non-linear behaviour of cancer risk curves in the low-dose region and question the validity of the Linear No-Threshold (LNT) model for cancer risk assessment through extrapolation from existing high-dose data [2-6].

Notwithstanding the proficient and active experimental activity in this field, many aspects related to low-dose phenomena remain still unclear nowadays, needing further investigations: above all, the mechanisms underlying these phenomena and their dependence on radiation quality, cell type and biological endpoint.

Moreover although a lot of experiments with living cells demonstrated that low-dose radiation can induce non-linear dose-dependent cell response, only few information regarding background radiation exposure of cryopreserved cells are available. Cell cryopreservation is an expedient to slow down the ageing process by halting their metabolic activity [7] taking profit of controlled low temperatures. Therefore this is a well-established procedure, which is routinely used in cell biology laboratories as well as in clinic practice, to store biological systems for future use. Due to the inhibition of cellular DNA repair mechanisms, it is expected that a multi-year exposure of frozen biological material (*i.e.* stem cells, embryos, sperms, cell lines etc.) to γ-ray environmental background can produce an accumulation of cellular damages over time and contribute to cancer or non-cancer pathology risk when such cells should be transplanted in individuals. Contrary to this hypothesis, preliminary data collected few years ago seem to indicate a protective effect of cryopreservation against the induction of radiation damage, in terms of different endpoints and in different biological systems [8].

In this framework, the multi-year EXCALIBUR (*EXposure effeCts At Low doses of Ionizing radiation in Biological CultURes*) experiment, funded by INFN-CNS5, has undertaken a multi-scale approach investigation on the biological effects induced in *in vitro* and *in vivo* biological systems, in culture and cryopreserved conditions, as a function of radiation quality (X/γ-rays, protons, He-4 ions of various energies) and dose, with particular emphasis on the low-dose region, in terms of different biological endpoints, including cell inactivation, apoptosis, cytogenetic damage, gene mutation, alterations of telomere length and ionic current flow as well as the role of nitrogen and oxygen reactive species in radiation-induced damage and signaling. The study is focused on the investigations of low-dose non-linear effects and, in particular, on Hyper-RadioSensitivity and Induced RadioResistance, HRS/IRR, bystander effects and genomic instability.

Moreover, the response to γ-rays of cryopreserved cells of different types and embryos is studied at different dose levels, mimicking the multi-year exposure of cryopreserved biological systems to the environmental γ-ray background, in order to clarify the protective effect of cryopreservation against the induction of radiation damage and in particular the role of some factors on the different response of cryopreserved systems with respect to living systems (*i.e.*: the low temperature; the presence and concentration of cryoprotectants, in particular the dimethyl sulphoxide, DMSO, which is known as a free radical scavenger).

In this contribution an account of the results obtained during the first year of the project are reported.

2. – Materials and methods

2˙1. *Biological systems.* – Cultured V79 Chinese hamster cells and AG1522 human foreskin fibroblasts were maintained in Dulbecco's modified Eagle's medium (D-MEM)

and α-MEM, respectively, supplemented with 10% heat-inactivated fetal bovine serum, antibiotics and L-glutamine.

Peripheral blood mononuclear cells (PBMCs) were isolated with Ficoll-Histopaque ($d = 1.077\,\mathrm{g/ml}$) from freshly collected blood samples of a healthy male donor (Transfusion Center of San Salvatore Hospital, Pesaro, Italy). For freezing, cells have been resuspended in a freezing solutions (50% FBS, DMSO 10%, 40% RPMI 1640), stocked into 2 ml vials with $2\text{–}5 \times 10^6$ cells/ml and frozen at $-196\,^\circ\mathrm{C}$ using a controlled rate freezer fed with LN (Nicool Plus PC, Air Liquide, Marne-la-Vallée, France).

ECV304 endothelial cells have been also used to evaluate the response of frozen and non-frozen cells to gamma irradiation

All cell lines were kept in incubator at 5% CO_2 humidified atmosphere at $37\,^\circ\mathrm{C}$.

Sheep embryos irradiated in cryopreserved condition and then transferred in recipient sheep have been used as *in vivo* biological system to evaluate the "protective" effect of cryopreservation against damage induced by γ-rays.

2˙2. *Cell irradiation.* – From 12 to 18 hours (depending on the cell line) before irradiation cells were plated as a monolayer on T25 flasks for X/γ-irradiation and on specially designed stainless-steel Petri dishes [9] for proton and alpha-particle irradiation.

Chinese hamster V79 cells were irradiated with Cs-137 γ-rays and broad beams of protons and alpha-particles of different energies in the dose range 0.1–5.0 Gy, depending on the biological endpoint to be analysed.

AG1522 cells were irradiated with 28.5 keV/μm protons, 62 keV/μm alpha-particles and X-rays in the dose range of 0.1–1 Gy.

Proton and alpha-particle irradiations were performed at the Radiobiology facility of the INFN-LNL 7MV Van de Graaff CN accelerator [9]. Proton energies of 0.8 MeV and 5 MeV, at the cell entrance surface (corresponding to LET values, in muscle tissue, of 28.5 keV/μm and 7.7 keV/μm, respectively) and alpha-particles of 8.4 MeV at the cell entrance surface (corresponding to LET values, in muscle tissue, of 62 keV/μm) have been used. All irradiation experiments were performed in the so-called track-segment conditions. Irradiation facility, beam dosimetry and irradiation modalities have been described in detail elsewhere [9, 10].

In order to investigate for bystander effect response, a "partial-shielding irradiation" system has been set up to prevent the irradiation of a fraction of the cell population. The partial sample shielding is obtained by placing a 200 μm thick tantalum foil upstream of the cell sample. For each irradiation experiment the percentages of irradiated and not-irradiated cell sub-populations are evaluated on the basis of the beam spots registered by GafChromic films, in partially shielded and unshielded geometries. In the cell irradiation experiments performed with 7.7 and 28.5 keV/μm protons the shielded sub-populations are in average $(35 \pm 2)\%$ of the whole population [11].

Experiments with X-rays were carried out by using a 250 kV, 6 mA apparatus equipped with a 0.2 mm copper filter (Gilardoni, Italy) as described elsewhere [10, 12]. Gamma irradiations (of living and frozen cells) were performed at Cs-137 gamma beams of the Department of Oncology (University of Padova), of S. Orsola University Hospital (University of Bologna) and San Salvatore Hospital (Pesaro).

Frozen cells were irradiated in vial. For V79 cells 3 vials were irradiated for each dose (0.5, 1 and 3 Gy).

Regarding irradiation of frozen and non-frozen PBMCs, to exclude cell death induced by freezing procedure and compare the effect of IR on frozen and non-frozen (fresh) cells, all samples were frozen. Briefly, PBMCs were directly irradiated at room temperature

and then immediately frozen or frozen and then irradiated in liquid nitrogen (LN) at −196 °C with different doses of γ-rays (0.3, 0.9 and 3 Gy). Unirradiated control samples were frozen as well.

Sham irradiated cells were used in all the experiments as control (unirradiated) cells.

2˙3. *Ionic current flow recordings, data acquisition and analysis in V79 cells.* – Membrane currents from ball-shaped V79 cells were measured in the whole-cell configuration of the patch-clamp technique at room temperature (22–24 °C) with an EPC-10 amplifier driven by the Patch Master software (HEKA Instruments, Darmstadt, Germany). Current traces were acquired at digitizing rates of 5–10 kHz and filtered at 2.9 kHz with an eight-pole low-pass Bessel filter. Voltage steps (20 mV, 100 ms) from −30 to 110 mV were delivered at intervals of 1 s; to inactivate other voltage-activated K^+ currents, the holding potential V_h was set to 0 mV [13]. Fast capacitance transients were minimized on-line by the patch-amplifier software which also performed, by global parameter setting (macro), a tracked leak compensation. This software setting allowed the automatic measurement of cell capacitance (C_m) and resting potential (V_m). The patch micropipette tip resistances ranged between 4 and 10 MΩ, when filled with electrode solution.

The bath solution (*p*H 7.4) contained (in mM): 133 NaCl, 4 KCl, 2 $MgCl_2$, 2 $CaCl_2$, 10 HEPES and 10 glucose. The electrode solution (*p*H 7.2) contained (in mM): 145 KCl, 1 $MgCl_2$, 1.8 $CaCl_2$ and 10 HEPES. Solutions containing 10 mM concentration of tetraethylammonium (TEA) were prepared from bath solution containing 123 mM NaCl. Unless otherwise stated, all chemicals and solutions were purchased from Sigma. Sodium and calcium currents were always prevented by adding 10 nM tetrodotoxin (TTX) to the bath solution. Stock solution of specific channels blockers (Alomone Labs, Jerusalem, Israel), were added to the bath and perfusing solutions at the required concentration before recording. Solutions were superfused at the rate of 1 ml/min trough a metallic cannula connected to a gravity-driven solution exchanger (VM8, ALA Scientific Instruments, Westbury, NY, USA) triggered by a TIB 14 interface (HEKA Instruments, Darmstadt, Germany) under the control of the Patch Master software.

Data are expressed as mean ± SEM Student's t-test was used to compute P values. A threshold of 0.05 was considered for statistical significance.

2˙4. *Telomere length alteration in AG1522 cells.* – After irradiation at different doses (0.1, 0.25, 0.5 and 1 Gy) AG1522 cells were detached and reseeded to be harvested 24, 48 and 72 hours later for the analysis of telomere "stickness", which are indicative of dysfunctions to telomeres structure/metabolism. Such telomeric alterations have been measured in anaphases in terms of frequency of chromosome bridges and bridges carrying telomeric signals (FISH analysis of PNA telomeric sequences). In fact, it is expected that in case of telomere length alterations or telomere dysfunctions, chromosome ends are "deprotected" and may interact with each other, giving rise to end-to-end fusions. The advantage of using fluorescent probes for telomeres in this kind of analysis is to monitor at anaphase and distinguish between chromosome bridges originating as a result of chromosome interexchanges (dicentric chromosomes), in which no telomere signals are expected to be present, and telomere-telomere fusions, where telomere signals are expected.

2˙5. *Cell survival of V79 cells.* – Cell survival has been used to test V79 cellular response after gamma and particles' irradiation, to investigate the possible presence of low-dose effects (hyper-radiosensitivity and bystander effect) as well as to study the radiation response of frozen and non-frozen cells.

TABLE I. – *Samples representative of the different components present in the frozen and cultured cells analyzed in the EPR measurements (see text). DMEM: Dulbecco's modified Eagle's medium; FBS: foetal bovine serum; DMSO: dimethyl sulphoxide.*

A1 : neat H_2O
A2 : H_2O + DMSO (10%)
A3 : complete DMEM
A4 : Complete DMEM + DMSO
A5 : Complete DMEM + FBS
A6 : Complete DMEM + FBS + DMSO (used for cryostorage)
A7 : V79 Cells in complete DMEM + FBS (15×10^6 total cells)
A8 : V79 Cells in thawing medium (15×10^6 total cells)
A9 : H_2O + FBS

Cell survival has been tested by colony-forming assay: after irradiation, for each dose point, including unirradiated control cells, V79 cells were washed with PBS buffer, trypsinized and counted, diluted with fresh medium and replated at appropriate concentration in 6 cm Petri dishes to determine the surviving fraction. After 7 days of growth at 37 °C, the cells were fixed and stained, and visible colonies with more than 50 cells were counted as survivors.

As regards frozen cells, after irradiation the frozen cells were thawed and then the same biological protocols as for the cultured cells was used for survival evaluations.

To investigate the different response to γ-rays of frozen and cultured V79 cells, cell survival has been measured in cell populations irradiated at different temperatures (−196, 0 and 37 °C), with and without DMSO.

2˙6. *EPR spectroscopy for radical yield evaluations.* – EPR spectroscopy of intermediate radicals of the radiation damage of cells and cell components stored in cryostatic conditions has been studied.

EPR measurements have been carried out on a series of samples representative of the different components present in the frozen and cultured cells (see table I) The samples have been submitted to gamma irradiation at 77 K in the dose range 0.15–7 kGy.

2˙7. *Apoptotic death on frozen and non-frozen PBMCs.* – After irradiation of frozen or non-frozen PBMCs, PBMCs were thawed and incubated for 0, 24, 48, 72 and 96 hours (37 °C and 5% CO_2) with or without phytohemagglutinin (PHA) stimulation; then cells were analysed by flow cytometry to evaluate the apoptotic process and cell cycle. Cells have been fixed in 70% cold ethanol, stained with propidium iodide and analysed with FACSCalibur flow cytometer (Becton-Dickinson, San Jose, CA, USA) [14]. The reported percentages were obtained on the basis of at least 40000 cells. Apoptotic cell death induced by ionising radiations (IR) typically involves DNA damaged cells and is revealed by the hypodiploid peak respect to diploid (on G0 phase of the cell cycle) living PBMCs (fig. 1).

Cell death of control (frozen, unirradiated) samples (spontaneous cell death) was used to calculate the percentage of specific cell death induced by IR as follows:

1) % of specific cell death=[% experimental cell death – % spontaneous cell death/ (100 –% spontaneous cell death)] × 100.

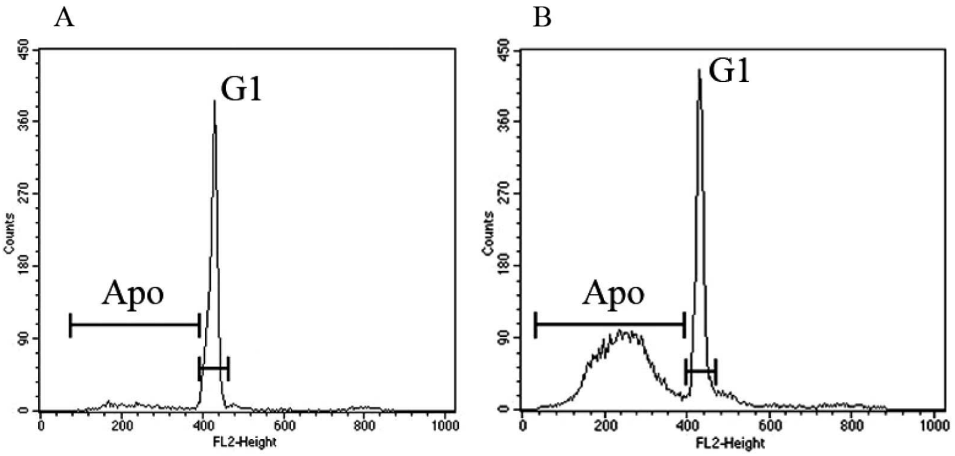

Fig. 1. – Panel A: PBMCs unirradiated (Control) (72 h incubation without stimulation); Panel B: PBMCs irradiated with 0.9 Gy (72 h incubation without stimulation). Apo: hypodiploid apoptotic cells; G1; living diploid PBMCs in G0/1 fase.

In the experiments in which, PBMCs (in G0 phase of cell cycle) were stimulated to proliferate with PHA, the cells in the phases S, G2 and mitosis were also estimated. To evaluate the inhibition of S-G2-M phases induced by gamma radiation, percentages of cycling cells were calculated within living cells (hypodiploid apoptotic cells excluded) as follows:

2) % of specific cycling cells (S-G2-M phases) = % of irradiated PBMCs in S-G2-M phases / % of unirradiated PBMCs in S-G2-M phases × 100.

Effect of irradiation in frozen and non-frozen ECV304endothelial cells have been also evaluated in terms of proliferation and intracellular ROS levels

3. – Results and discussion

3˙1. *Ion current flow recordings, data acquisition and analysis in V79 cells*. – Potassium channels in V79 cells were characterized by using the blocker tetraethylammonium (TEA). The current reduction after perfusion with TEA (fig. 2) clearly indicates that the channels are potassium channels. A dose– and radiation-type–dependent reduction in the potassium currents was observed.

I-V curves were obtained, where V is the applied potential and I the elicited current, as described in the methods section.

In particular, the exposure with alpha-particles resulted statistically significant ($P < 0.05$) if compared to control (not exposed cells) also for low doses (0.5 Gy) for those potential values that elicited the maximal current (high values of V) and resulted statistically significant for all the stimulating potentials for a dose of 2 Gy.

The exposure with protons, at doses between 0.25 and 0.50 Gy, resulted on the borderline of statistical significance ($P = 0.05$), whereas for higher doses (1, 2, and 4 Gy), resulted significantly different ($P < 0.05$).

The exposure with γ-rays was performed at 0.5, 1, 2, 6.5 e 12 Gy, and significant reduction in potassium currents was observed for doses higher than 1 Gy.

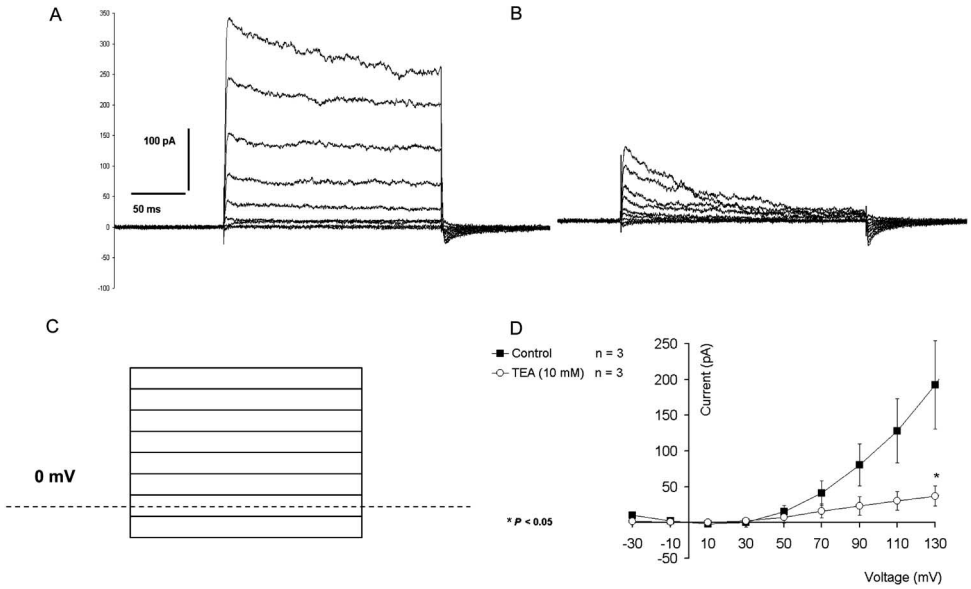

Fig. 2. – TEA effect on outward currents recorded in whole-cell configuration in murine fibroblasts immortalized V79. Representative examples of current traces recorded in the same cell before (A) and after 10 mM TEA application (B). (C) Graphical representation of the pulse protocol (holding potential at 0 mV). Steps of +20 mV are applied every 1 s from −30 mV to +130 mV. (D) Average of current-voltage relationships (I-V) before and after TEA application. * denotes $P < 0.05$ with Student's t-test.

Potassium (K^+) channels are expressed in a wide range of mammalian cells. In excitable cells such as neurons and muscles, K^+ channels play a critical role in the maintenance of the resting membrane potential and in the regulation of action potential generation and repolarisation, pacemaking and neurotransmitter release [15]. In non-excitable cells, K^+ channels are involved in volume regulation, hormonal secretion, cell proliferation and apoptosis, and are cell-cycle regulated [16, 17] These channels are ubiquitously distributed among different cell types, and play a tissue- and cell-specific role in pH homeostasis, cell differentiation, neuroendocrine secretion and signal transduction [18, 19] The observation of K^+ current in V79 cells is, the first characterization of this type of channels in these cells. The observed reduction in K^+ current, following ionizing radiation exposure, may indicate a secondary effect, generated from an increase of free radical concentration as well as an alteration in the cell cycle and in the cellular proliferative capability.

Moreover it can be argued that in general, the dose-response curves show similar monotone- decreasing trends with non-linearity at low doses, whereas, for higher doses (starting from 2 to 4 Gy) they reach a plateau.

3˙2. *Telomere length alteration on AG1522 cells.* – Data obtained show a dose-dependent response in the frequency of anaphase bridges observed 24, 48 and 72 hours from the exposure to both the radiation type, though helium ions showed an higher effectiveness in the induction of such kind of cytogenetic endpoint, compared with protons and X-rays. As a function of harvesting times, the frequency of bridges declined for both

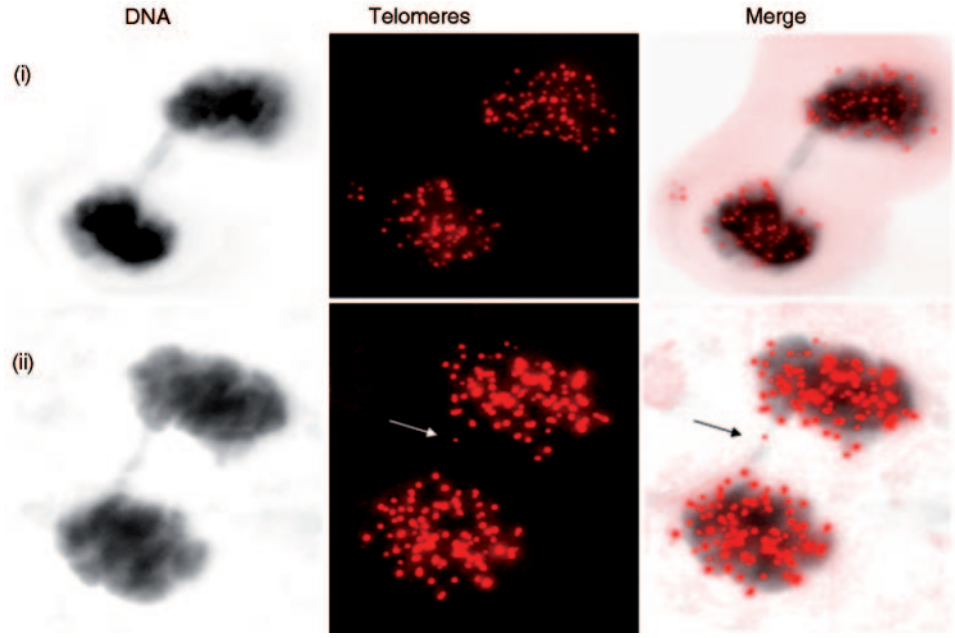

Fig. 3. – Representative images of anphases displaying chromosome bridges with (ii, arrow) and without (i) telomere signal.

types of radiations, though for high-LET radiations, that is protons and helium-ions, a higher persistence of bridges was detected in comparison with X-rays. The role of telomere in the formation of such anaphase bridges, remains to be investigated in detail in a larger sample, since the frequency of telomere signals as evaluated by FISH analysis on bridges in anaphases (fig. 3), were rather low irrespective of the type of radiation. Overall, these data seem to indicate that radiation-induced telomere alterations play only a minor role in the generation of anaphase bridges for low- as well as for high-LET radiations, and the majority of bridges are the result of unstable structural aberrations. Therefore a different approach was used to further clarify this aspect.

As previously mentioned, non-linear effects have been provided not only for cell killing, but also reported for chromosome aberrations, as shown by using classical cytogenetic techniques (Giemsa staining). The use of such methods of staining, however, requires the analysis of a very high numbers of methaphases and is not suitable to ascertain the induction of stable aberrations, such as chromosome translocations. In addition, the low-dose effect in terms of hypersensitivity to low dose, seems not to be simply related to the LET of the radiation used. In fact, at least for cell survival experiments, it seems that hypersensitivity to radiation is rather linked to radiation type than simply to LET. In addition, telomere alterations are known to play a role in chromosome aberration formation, and therefore it is worth to analyse the relationship between radiation-induced telomere alterations and the yield of structural chromosomal rearrangements.

To study both these topics, AG1522 fibroblasts have been irradiated and calyculin-A–induced metaphases collected after 24 hours for the evaluation of cytogenetic damage by means of the powerful technique of M-FISH (Multicolour FISH). This method of staining allows to detect chromosome aberrations on the whole genome by means of

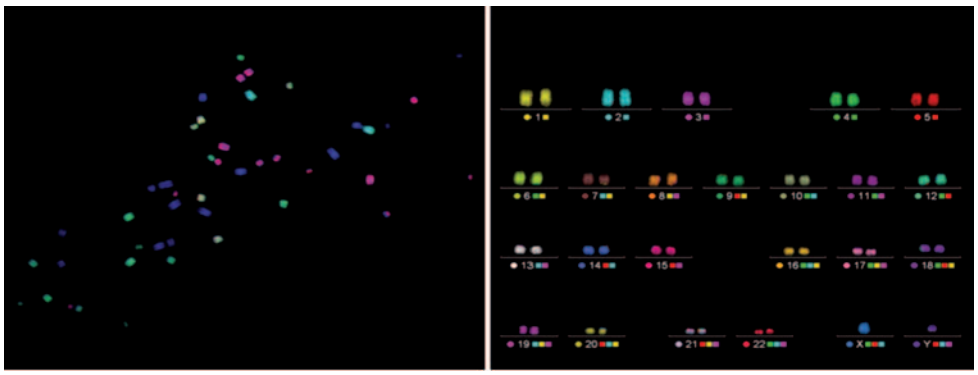

Fig. 4. – An example of AG1522 M-FISH–painted chromosomes.

specific probes for the different chromosomes at once (fig. 4). A multi-filter–equipped fluorescence microscopy, a CCD camera and a dedicated software are used during the analysis. So far, cells have been irradiated in the 0.1–1 Gy dose range of 3 MeV protons and X-rays.

3˙3. *Cell inactivation in V79 cells*. – Cell survival curves have been measured at graded doses (0.1–4 Gy) in V79 Chinese hamster cells, after 7.7 and 28.5 keV/μm protons (primary beam energy of 6 and 3 MeV, respectively). Cell samples have been irradiated in "broad beam" and in "partial shielding" geometry to investigate the HyperRadioSensitivity and Induced RadioResistance (HRS/IRR) and Bystander Effect (BE) occurrence, respectively. No clear evidence of HRS/IRR and of a consistent BE response can be identified in the low-dose region of V79 survival curves after proton irradiation of both energies. The lack of HRS/IRR in V79 cells after proton irradiation has been observed also in terms of chromosomal aberration and micronuclei induction, in contrast with results obtained after gamma irradiation where HRS/IRR has been shown below a dose level of 0.5 Gy in terms of cell survival, chromosomal aberration and micronuclei induction. However it should be underlined that cytogenetic data after proton irradiation come from two experiments and therefore are preliminary, and need to be confirmed with additional replicates.

Cell survival and Hprt mutation induction in V79 cells after gamma irradiation have been measured at graded doses (0.5–3 Gy) as a function of temperature (at 0 °C and 37 °C temperatures) and DMSO concentration (with and without DMSO), to be compared with the response of cryopreserved cells to radiations in order to get insight into the role of the DMSO (ROS scavenger). Preliminary results on V79 cell survival seem to indicate that the presence of DMSO produces a more significant effect in cell inactivation than the temperature.

3˙4. *Apoptotic death in peripheral blood mononuclear cells*. – Apoptotic cell death of frozen PBMCs induced by γ-rays increases with time and dose of radiation on PBMCs cells cultured without mitogenic stimulation (fig. 5). On the other hand, PHA stimulation of frozen PBMCs inhibits the specific cell death induced by gamma radiation compared to unstimulated samples (fig. 6). Differently from PBMCs irradiated at room temperature, inhibition of cell cycle entry after PHA stimulation induced by γ-rays was usually lower than in frozen PBMCs (fig. 7). Interestingly, irradiation of frozen PBMCs produces

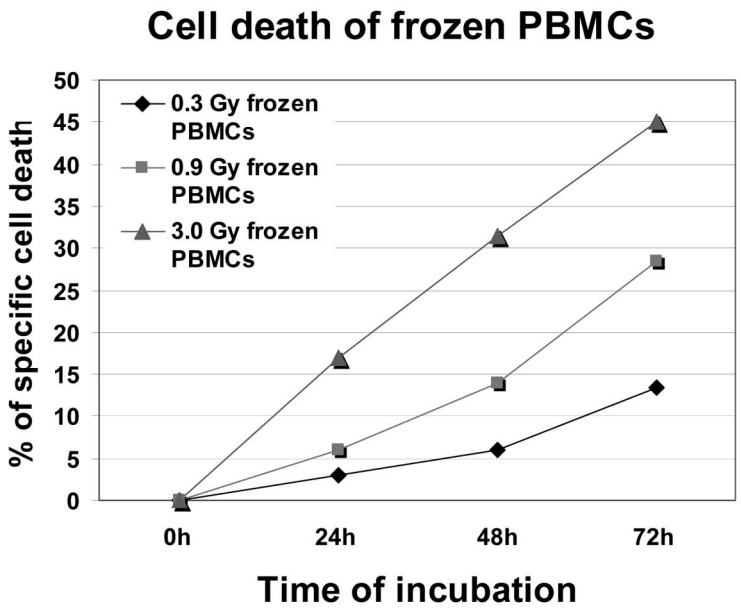

Fig. 5. – Specific cell death of PBMCs irradiated, frozen and cultured without stimulation. Evaluation of specific cell death on frozen irradiated PBMCs at the indicated radiation doses and incubation times without stimulation. A representative experiment.

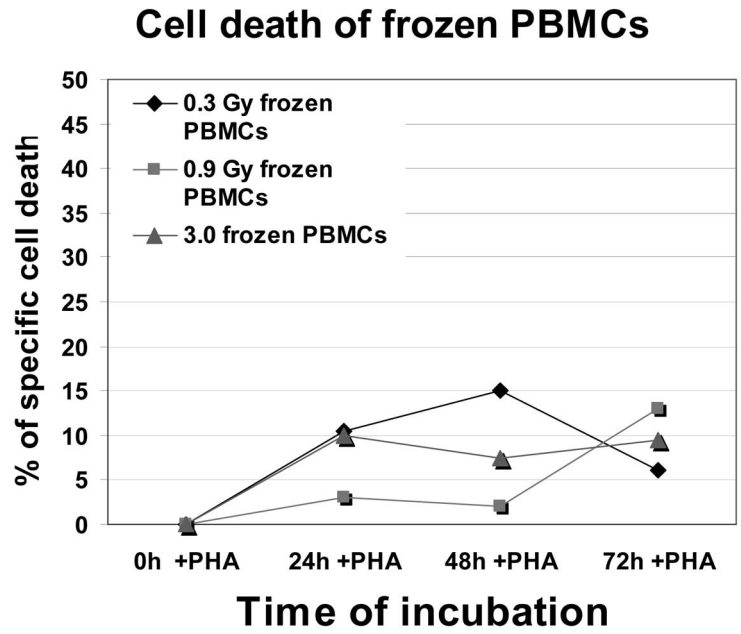

Fig. 6. – Specific cell death of PBMCs irradiated, frozen and then cultured with PHA. Evaluation of specific cell death on frozen irradiated PBMCs at the indicated radiation doses and incubation times after PHA stimulation. A representative experiment.

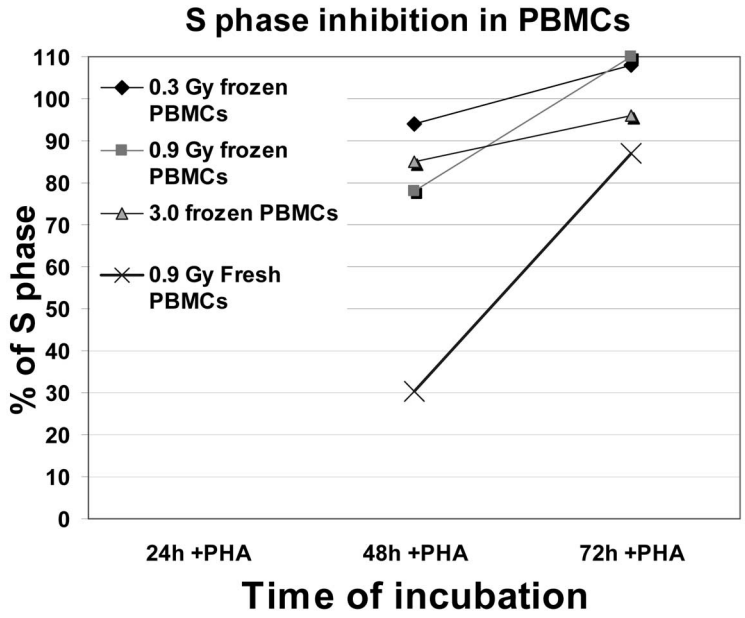

Fig. 7. – Percentages of cycling PBMCs irradiated, frozen or at room temperature and then cultured with PHA. Percentages of cycling cells (S-G2-M phases of cell cycle) with unirradiated control PBMCs equal to 100%. A representative experiment.

a lower percentage of apoptotic cells compared to fresh PBMCs irradiated with the same dose at room temperature and then frozen (fig. 8).

In frozen PBMCs, cell survival progressively decreased with dose radiation and incubation time, and tended to disappear below 0.3 Gy dose radiation. These observations were not confirmed in PHA-stimulated samples. Indeed, stimulation of frozen PBMCs with PHA seems to favour cell survival and/or to mask radiation-induced cell death (PHA significantly increases cell death of samples.) Moreover, inhibition of cell cycle induced by γ-rays in PHA-stimulated samples was not a sensitive marker of cell perturbation in frozen PBMCs. Interestingly, percentages of specific cell death in PBMCs irradiated in liquid nitrogen with 0.9 Gy were lower than those of samples irradiated at room temperature, indicating that the frozen state protects from ionising radiation. These observations are in agreement with previous reports [20, 21] and might depend on the block of free radicals produced by low temperatures [22, 23] or on the impairment of apoptosis-inducing mechanisms.

3˙5. *Proliferation and ROS levels in frozen and unfrozen ECV304 cells.* – The effects of irradiation has been evaluated on proliferation and intracellular ROS levels in frozen and unfrozen human endothelial cells (ECV304). Cells were irradiated with 0.4, 0.8, 1.2, 2.4, 3.2, 4.8 and 8 Gy and intracellular ROS levels were assessed 1, 4, 8 and 11 days after irradiation. Results from three different measurements show no significant differences in intracellular ROS levels between treated and untreated cells, indicating that ROS decay in short time after irradiation. Data from cell count experiments, performed at the same time of ROS measurements, significantly indicated that the frozen cells seem to be more resistant to high irradiation doses as compared to the unfrozen ones. Future experiments

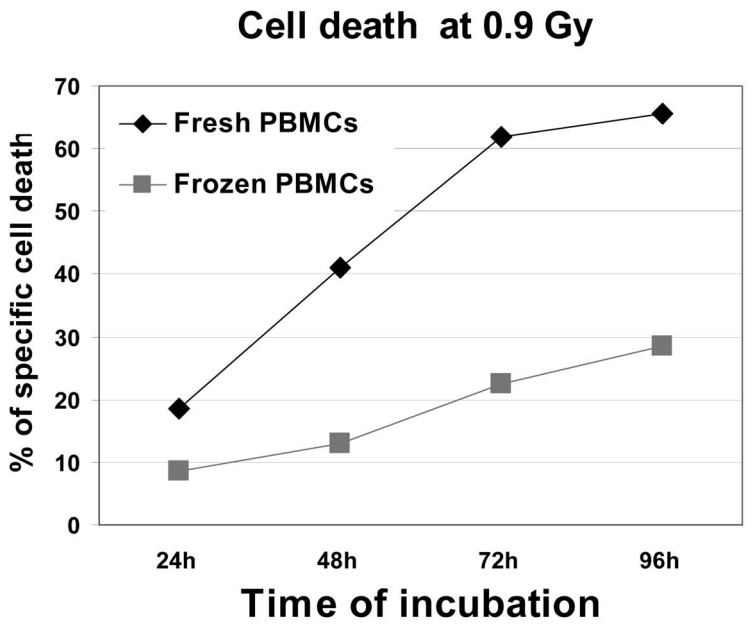

Fig. 8. – Inhibition of cell death of PBMC irradiated in the frozen state compared to irradiation at room temperature. Specific cell death percentages of PBMCs irradiated with 0.9 Gy at room temperature or at −196 °C. A representative experiment.

will be aimed at evaluating cell proliferation and intracellular ROS level in both frozen and unfrozen cells soon after irradiation.

3˙6. *Follow up of lambing obtained from irradiated embryos.* – Three different dose levels of γ-rays (0.3, 2.4, 19.2 Gy) were used to irradiate *in vitro* produced vitrified (cryopreserved) sheep embryos.

The embryos after warming were transferred into recipient sheep. Lambs born were monitored by cytofluorimetric analysis to evaluate blood values. The grown-up lambs were monitored for body and health parameters until the first pregnancy and lambing. The irradiated male lambs were used to fertilise the irradiated females.

3˙7. *Radical yield measurements in frozen samples.* – The total radical yield is approximately linear with the dose and in the dose range exploited no significant changes were observed concerning the nature and distribution of the radical products

The possibility of extending the EPR measurements at the dose range < 1 Gy has been assessed. For this purpose, the sensitivity of the measurements had to be enhanced by implementing the spectra accumulation system.

A drastic decrease of the EPR signal from OH-radicals was observed in the samples containing DMSO. This result has been associated with the formation of glass phases. It is being investigated whether this effect stems from a real decrease of the OH-radical concentration or it is a physical EPR effect due to the loss of symmetry of the H bond systems in the glassy phase OH-radicals to a lower extent HO_2-radicals are dominant in pure water and are present in all types of samples.

Such species decay at 140 K without giving rise to new EPR signals. This lack of evidence for the interaction of OH-radicals with the organic components and cells in the

frozen mixtures has partly been explained with the crystalline ice phase segregation. The confinement of radical species as OH-radicals in separated phases formed on freezing is a major source of differences with respect to radiolysis in the liquid state.

CH_3-radicals from DMSO are already present after the irradiation at 77 K. Such species can be thought to arise from direct radiolysis as well as from scavenging of mobile species as H-atoms and electrons. As CH_3-radicals are quite mobile and reactive toward organic substrates, it is likely that the protective effect of this DMSO be related to its attitude to favour glass phase formation and not to its radical scavenging properties

The main species detected in A2–A8 samples (table I) are generated by direct radiolysis of the specific components with a yield greater than that of radicals in pure water. Such species are stable at 77 K and no appreciable changes are observed up to 140 K. It is reasonable to expect that such species can transfer their radical damage to other components only on melting. Most of the radical species decay at $T < 200$ K lower than that obtained from the DMSO/water phase diagram.

This phenomenon can be reckoned with premelting due to glass phases.

The results have afforded evidence of the role of the phases in determining the lifetime and the reactivity of free radicals produced during the irradiation at 77 K and the radical damage transfer to cell system and organic substrates on melting. Radical yields and kinetic measurements in DMSO/H_2O binary systems of variable composition have been initiated in connection with the phase diagram obtained from the literature. The problem of extending the sensitivity of the EPR measurements to low doses has been solved by enhancing the spectra accumulation system of the spectrometer.

* * *

This work was supported by INFN funds for EXCALIBUR project. AL is the recipient of a Ph.D fellowship from Associazione Sammarinese Leucemie ed Emopatie Maligne (ASLEM). LZ is grateful to Drs. B. Canonico, F. Luchetti, M. Arcangeletti, M. D'Atri and F. Bastianelli for technical assistance and to Prof. S. Papa for his continuous interest and advice.

REFERENCES

[1] García-Talavera M., Matarranz J. L., Martínez M., Salas R. and Ramos L., *Radiat. Prot. Dosim.*, **124** (2007) 353.
[2] Mothersill C. and Seymour C., *Radiat. Res.*, **155** (2001) 759.
[3] Hall E. J., *Health Phys.*, **85** (2003) 31.
[4] Morgan W. F., *Radiat. Res.*, **159** (2003) 567.
[5] Prise K. M., Folkard M. and Michael B. D., *Radiat. Prot. Dosim.*, **104** (2003) 347.
[6] *Health Risks from Exposure to Low Levels of Ionizing Radiation: BEIR VII Phase 2* (The National Academies Press) 2006.
[7] Mazur P., *Am. J. Physiol.*, **247** (1984) C125.
[8] Bottigli U., Brunetti A., Carpinelli M., Diaz N., Fiori P. L., Golosio B., Masala G. L., Oliva P., Randaccio P., Santona S., Zamai L., Centis F., Valentini M., Cesarini W., Canonico B., Grianti F., Balata M., Nisi S., Laubenstein M., Papa S., Bedogni R., Esposito A., Cherubini R., De Nadal V. and Gerardi S., *Nuovo Cimento C*, **31** (2008) 11.
[9] Belli M., Cherubini R., Galeazzi G., Mazzucato S., Moschini G., Sapora O., Simone G. and Tabocchini M. A., *Nucl. Instrum. Methods Phys. Res. A*, **256** (1987) 576.

[10] Sgura A., Antoccia A., Cherubini R., Dalla Vecchia M., Tiveron P., Degrassi F. and Tanzarella C., *Int. J. Radiat. Biol.*, **76** (2000) 367.
[11] Cherubini R., De Nadal V., Gerardi S., Guryev D., Antoccia A., Berardinelli F., Sgura A. and Tanzarella C., *Nuovo Cimento C*, **31** (2008) 57.
[12] Sgura A., Antoccia A., Cherubini R. and Tanzarella C., *Radiat. Res.*, **156** (2001) 225.
[13] Nishimaru K., Eghbali M., Lu R., Marijic J., Stefani E. and Toro L., *J. Physiol.*, **559** (2004) 849.
[14] Zamai L., Falcieri E., Gobbi P., Santi S., Falconi M., Marhefka G. and Vitale M., *Cytometry*, **25** (1996) 324.
[15] Hille B., *Ionic Channels of Excitable Membranes* (Sinauer Associates Inc., Sutherland) 1992.
[16] Nilius B. and Droogmans G., *Physiol. Rev.*, **81** (2001) 415.
[17] Pardo L. A., *Physiology*, **19** (2004) 285.
[18] Lu R., Alioua A., Kumar Y., Eghbali M., Stefani E. and Toro L., *J. Physiol.*, **570** (2006) 65.
[19] Wu S.-N., *Curr. Med. Chem.*, **10** (2003) 649.
[20] Ashwood-Smith M. J. and Grant E., *Ciba Found. Symp.*, **52** (1977) 251.
[21] Ashwood-Smith M. J. and Friedmann G. B., *Cryobiology*, **16** (1979) 132.
[22] Garman E., *Curr. Opin. Struct. Biol.*, **13** (2003) 545.
[23] Yasui L. S., *Int. J. Radiat. Biol.*, **80** (2004) 895.